Cellular Activity on Titania Nanotube Surfaces by Non-thermal Atmospheric Pressure Plasma with Different Gas

Hye-Yeon Seo

Department of Dentistry

The Graduate School, Yonsei University

Cellular Activity on Titania Nanotube Surfaces by Non-thermal Atmospheric Pressure Plasma with Different Gas

Directed by Professor Kyoung-Nam Kim

The Doctoral Dissertation
submitted to the Department of Dentistry,
the Graduate School of Yonsei University
in partial fulfillment of the requirements for the degree of
Ph.D. in Dental Science

Hye-Yeon Seo

June 2015

This certifies that the Doctoral Dissertation of 'Hye-Yeon Seo' is approved.

Thesis Supervisor : Kyoung-Nam Kim

Thesis Committee Member#1 : Kwang-Man Kim

Thesis Committee Member#2 : Seong-Ho Choi

Thesis Committee Member#3 : Sang-Bae Lee

Thesis Committee Member#4 : Eun Ha Choi

The Graduate School

Yonsei University

June 2015

감사의 글

박사논문을 무탈하게 완성할 수 있도록 음양으로 도와주신
모든 분들께 감사 드립니다.

박사논문을 완성한 지금, 그간의 시간을 되돌아 보니 감동과 성취감에 젖은 석사 때와 달리 책임감이 가중되어 많은 생각이 듭니다. 앞으로 저에게 주어지는 모든 것에 감사하고, 그것을 인정하며 '아쉬움은 남아도 후회는 없는 삶'을 만들어가라는 아버지의 말씀처럼 주어진 임무에 의무를 다하겠습니다.

저의 지도교수님이신 김경남교수님. 교수님의 제자로 남을 수 있어 기쁘고 영광입니다. 임신, 출산, 육아까지 세심하게 챙겨주시고 저의 상황을 배려해주셔서 논문을 완성할 수 있었습니다. 스승의 은혜 마음속 깊이 간직하겠습니다. 김광만 교수님, 제가 생각하지 못한 부분을 다정다감하게 조언해 주시고, 보다 나은 결과를 도출할 수 있도록 이끌어 주셔서 감사 드립니다. 저의 논문을 위해 참되고 성실한 마음과 뜻을 다하여 지도해주신 이상배 박사님, 최성호 교수님, 최은하 교수님께 감사한 마음 전합니다. 그리고 본 학위논문의 연구진행과 실질적인 실험에 애써주신 권재성, 최유리, 이은정 선생님 향후 어떠한 형태로든 꼭 보답하겠습니다. 고맙습니다. 제가 교실에 잘 적응 할 수 있도록 보살펴 주신 따뜻한 유은미, 최혜숙교수님 감사합니다. 그리고 치과생체재료공학교실 모든 선생님들 제가 학교생활 무리 없이 이어나갈 수 있도록 하나부터 열까지 도와주셔서 진심으로 감사하고, 앞으로 하시는 일 모두 잘 되시길 축원합니다.

제가 좋아하는 연하회, 행원, DMDH 교수님과 선생님들. 우리 가고자 하는 길은 달라도 서로 손잡고 지지해주며 함께 나아가요.

아버님, 어머님. 아직 채워야 할 것이 너무나도 많은 저를 지지해주시고 믿어주셔서 감사합니다. 두 분의 사랑을 느낄 수 있어 행복하고, 제2의 부모님이 되어주신 날부터 저는 천군만마를 얻은 것보다 더 든든합니다. 사랑합니다.

그리고 30년 만에 나타난 제가 너무너무 좋아하고 의지하는 우리 지경언니. 늘 저의 편이 되어줘서 고맙습니다. 그리고 포근한 아주버님과 한 가족이 되어 기쁩니다. 한 가족의 구성원으로 서로 공감하며, 행복한 인생 만들어 나가시길 바랍니다.

우리 최강우애 서남매 승혜 그리고 준태야. 너희 둘은 부모님께서 나에게 주신 가장 큰 선물이야. 사랑하고 사랑하고 사랑해.

사랑한다는 말로는 턱없이 부족한 내 인생 최고의 네잎클로바 남편님. 석사 때 만나서 박사 시작할 때 결혼하고 현재는 아들까지 둔 행복한 가정을 안겨준 그대, 최고의 행복지수를 선사해주는 그대에게 존경하는 마음과 감사한 마음을 표합니다.

용감하고 씩씩하고 정의로운 우리 준민아. 엄마아들로 태어나줘서 고맙다. 우리 준민이가 진심으로 엄마를 사랑하고 닮고 싶은 사람이 되도록 노력하마. 사랑한다.

마지막으로 형용할 수 없는, 그 무엇으로도 대체할 수 없는 사랑하는 아빠 그리고 엄마. 박사를 마무리하는 현 시점에서 가장 생각나고 감사한 분은 아빠엄마예요. 두 분의 딸로 태어나 행복한 인생을 살게 해주셔서 감사하고 사랑합니다. 제 인생의 원동력이 되어주신 부모님께 이 논문을 바칩니다.

2015. 6. 서혜연 올림.

TABLE OF CONTENTS

LIST OF FIGURES

LIST OF TABLE

ABSTRACT

Cellular Activity on Titania Nanotube Surfaces by Non-thermal Atmospheric Pressure Plasma with Different Gas

Hye-Yeon Seo

Department of Dentistry

The Graduate School, Yonsei University

(Directed by Professor Kyoung-Nam Kim, D.D.S., Ph.D.)

The surface topography and chemistry of titanium implants are important factors for successful osseointegration. However, chemical modification of an implant surface using currently available methods often results in the disruption of topographical features and the loss of beneficial effects during the shelf life of the implant. Therefore, the aim of this study was to apply the recently highlighted portable non-thermal atmospheric pressure plasma jet (NTAPPJ), elicited from one of two different gas sources (nitrogen and air), to TiO_2 nanotube surfaces to further improve their osteogenic properties while preserving the

topographical morphology. The surface treatment was performed before implantation to avoid age-related decay. The surface chemistry and morphology of the TiO_2 nanotube surfaces before and after the NTAPPJ treatment were determined using a field-emission scanning electron microscope, a surface profiler, a contact angle goniometer, and an X-ray photoelectron spectroscope. The MC3T3-E1 cell viability, attachment and morphology were confirmed using calcein AM and ethidium homodimer-1 staining, and analysis of gene expression using rat mesenchymal stem cells was performed using a real-time reverse-transcription polymerase chain reaction. The results indicated that both portable nitrogen and air based NTAPPJ could be used on TiO_2 nanotube surfaces easily and without topographical disruption. NTAPPJ resulted in a significant increase in the hydrophilicity of the surfaces as well as changes in the surface chemistry, which consequently increased the cell viability, attachment and differentiation compared with the control samples. The nitrogen-based NTAPPJ treatment group exhibited a higher osteogenic gene expression level than the air-based NTAPPJ treatment group due to the lower atomic percentage of carbon on the surface that resulted from treatment. It was concluded that NTAPPJ treatment of TiO_2 nanotube surfaces results in an increase in

cellular activity. Furthermore, it was demonstrated that this treatment leads to improved osseointegration *in vitro*.

Key words: non-thermal atmospheric pressure plasma, TiO_2 nanotube, osseointegration, nitrogen, air

Cellular Activity on Titania Nanotube Surfaces by

Non-thermal Atmospheric Pressure Plasma with Different Gas

Hye-Yeon Seo

Department of Dentistry

The Graduate School, Yonsei University

(Directed by Professor Kyoung-Nam Kim, D.D.S., Ph.D.)

I. Introduction

1. Nanostructure surfaces

The implant method as a way of restoring the lost tooth is getting diversified (Albrektsson and Wennerberg, 2005). Titanium (Ti) is commonly used for medical and dental implants, for which surface modifications involving the chemical composition, energy level, morphology, topography and roughness have been widely studied (Rupp *et al.*, 2006). Among these factors, the surface topography and chemistry of Ti implants are known to be important for successful osseointegration (Klokkevold *et al.*, 1997; Kim *et al.*, 2006). Though results were influenced by experimental design, including sample preparation method, sterilization and cell type as shown by Faghini *et al.*

(2006), Wirth *et al*. (2008), and Chien *et al*. (2008). The implant surface topography has been known to be the main influencing factor on osteoblastic cell adhesion and fibroblast responses (Anselme and Bigerelle, 2006; Le Guehennec *et al.*, 2007; Meredith *et al.*, 2007), where topographical modifications of the implants surfaces have been attempted to improve the integration of hard and soft tissues (Wennerberg and Albrektsson, 2010). Recently, nanostructure surfaces such as titania (TiO_2) nanotubes have been studied because the topographical modifications that were reported to be superior in early biological events related to the adsorption of proteins, blood clot formation and cell behavior (Lavenus *et al.*, 2010), all resulted in a higher degree of osseointegration (Ellingsen *et al.*, 2004).

Well-developed filopodia directly entered nanometer-sized pores for the initial attachment of the osteoblastic cells. These nanometer structures may also give the cells positive guidance by means of the selective attachment of osteoblasts to the implant surface (Le Guéhennec *et al.,* 2007). In particular, previous studies reported that large-diameter TiO_2 nanotubes had favorable osteogenic properties, were non-cytotoxic, maintained a nanoporous surface that were highly beneficial for bio-implants (Uhm, 2013).

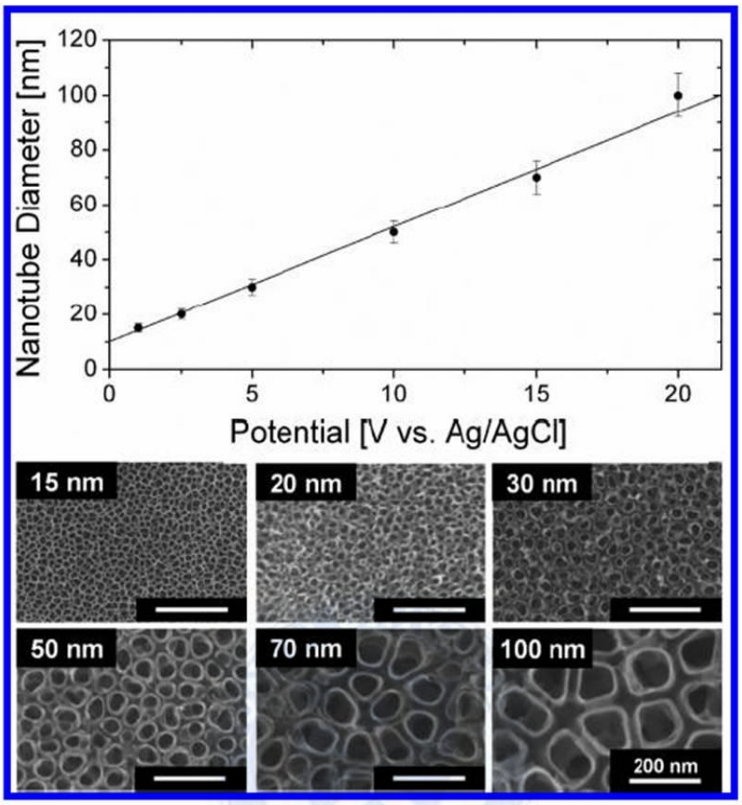

Figure 1. Surface of layers of self-aligned TiO_2 nanotubes with different diameters. Self-assembled layers of vertically oriented TiO_2 nanotubes were generated by anodizing titanium sheets. SEM images show highly ordered nanotubes of six different pore sizes between 15 and 100 nm created by controlling potentials ranging from 1 to 20 V (Park *et al.,* 2007).

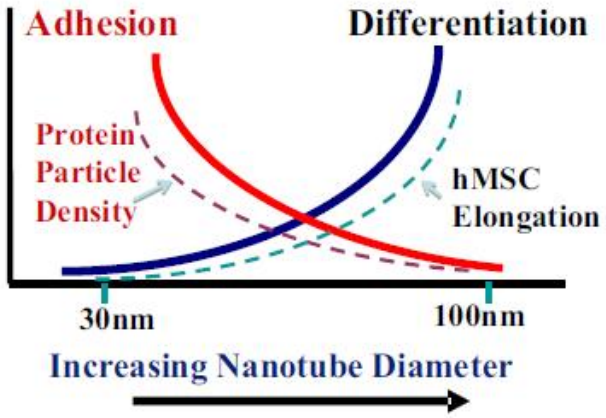

Figure 2. Schematic illustration of the overall trends of nanotube effects on hMSC fate and morphology after a 24-h culture. The change in hMSC cell adhesion and growth without differentiation (solid red line) has the same trend as protein particle density (broken red line), whereas that of differentiation (solid blue line) has the same trend as hMSC elongation (broken blue line) (Oh, 2009).

2. Chemistry of osseointegration

Surface chemistry is another major factor to influence the response of osteoblst cells to the implant.

This biological fixation is considered to be a prerequisite for implant-supported prostheses and their long-term success. The rate and quality of osseointegration in titanium implants are related to their surface properties. Surface composition, hydrophilicity and roughness are parameters that may play a role in implant–tissue interaction and osseointegration (Le Guéhennec *et al*., 2007).

Certain cell bioactivity is more affected by the surface chemistry than by the surface topography (Anselme and Bigerelle, 2006), as observed in recently developed highly hydrophilic implant surfaces with better osseointegration than conventional surfaces (Swase *et al*., 2008). Also the effects of plasma on Ti surfaces have been widely studied for the modification of surface roughness, wettability and cell-surface interactions (Ikeda, 2002; Shibata, 2002; Kawai, 2004).

Despite many attempts to modify the chemical features of Ti surfaces, the time-dependent degradation of the chemical effects is substantial in that the strength of osseointegration is reduced with aged Ti surfaces compared with newly prepared Ti surfaces (Lee and Ogawa, 2012).

Additionally, chemical modifications with a high-energy vacuum

environment often result in the disruption of beneficial topographical features in biomaterials (Fridman, 2008). Osteoblast-cells cultured on these chemically purer and hydrophilic surfaces produced more differentiation markers represented by increased cell layer alkaline phosphatase specific activity and osteocalcin; and created an osteogenic microenvironment by increasing local factors (Zhao *et al.*, 2005).

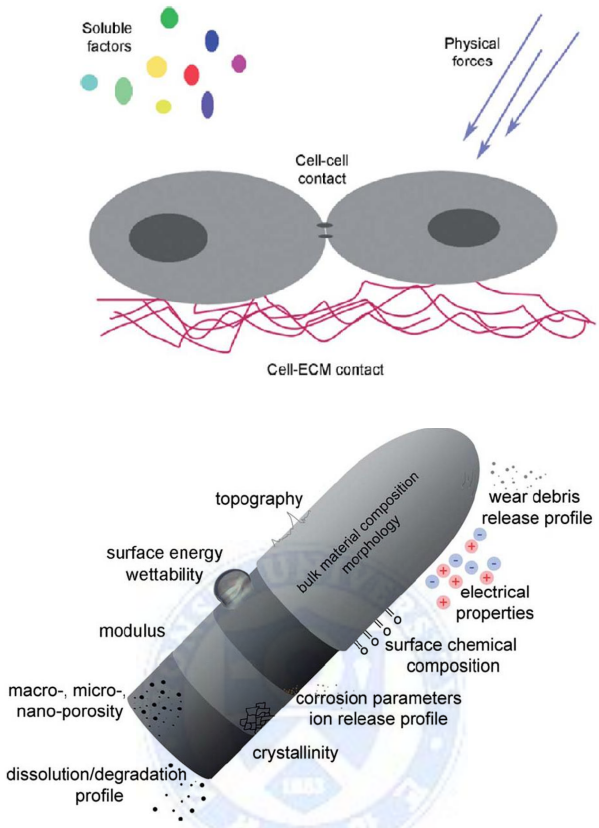

Figure 3. Factors influencing stem cell differentiation and major material variables that could influence the host response (Kaivosoja E *et al.,* 2012).

Table 1. Some effects of different surface chemistries on proteins and stem cells.

Functional group	Properties	Effect on proteins and stem cells
-CH	Neutral; hydrophobic	Has high affinity/binding with fibrinogen; supports MSC maintenance
-OH	Neutral; hydrophilic	Has relatively low affinity for plasma proteins, induces exposure of cell adhesive domains on fibronectin , does not support long-term adipogenic differentiation, promotes chondrogenic differentiation
-NH2	Positive; hydrophilic	Has high affinity for fibronectin, most favourable for osteogenic differentiation
-COOH	Negative; hydrophobic	Has increased affinity for fibronectin and albumin, promoted chondrogenic differentiation

Kaivosoja E *et al*., 2012.

3. Non-thermal atmospheric pressure plasma

Non-thermal atmospheric pressure plasma has been recently applied in many biological fields with the advantages of being low in temperature such that it can be used on biomaterial surfaces without resulting in changes in the topography (Kalghatgi, 2011). Atmospheric-pressure non-thermal plasma-jet has been an emerging field which has been actively applied to resolve various medical problems such as treatment of skin diseases, dental cavities, control the contamination of various surfaces, promote cell proliferation, enhance cell transfection, wound healing, and ablate the cultured cancer cells (Kumar, 2014).

Additionally, the atmospheric pressure plasma device does not require a vacuum environment (Duske *et al.*, 2012), making it portable for the treatment of biomaterial surfaces directly before their application. The plasma treatment of biomaterials is known to render surfaces hydrophilic and to modify the oxide layer that interacts with the proteins and cells of surrounding tissue, which leads to an increased adhesion of cells and tissue compared with plasma untreated samples (Schwarz *et al.*, 2008; Duske *et al.*, 2012). One of the most popular non-thermal atmospheric pressure plasma sources are based on dielectric barrier discharges type which previously have been applied to biomaterials in many studies (Bardos L. and Barankova H, 2010). However, there has not been study that applied NTAPPJ on TiO_2 nanotubes.

4. Research objectives

The purpose of this study was to apply a non-thermal atmospheric pressure plasma jet (NTAPPJ) with different gas sources to potentially surface treat nanotube dental implants directly before surgery to improve their hydrophilicity and osteogenic properties to avoid the withering of the benefits of chemical modification while preserving the topographical morphology.

The Null hypotheses of study were as follows:

Null hypothesis 1: In the treated and untreated with NTAPPJ, there would be no difference in physical properties.

Null hypothesis 2: In the treated and untreated with NTAPPJ, there would be no difference in chemical properties.

Null hypothesis 3: In the treated and untreated with NTAPPJ, there would be no difference in biological properties.

Null hypothesis 4: The effect of physical, chemical, biological would not be affected by the different plasma gas sources.

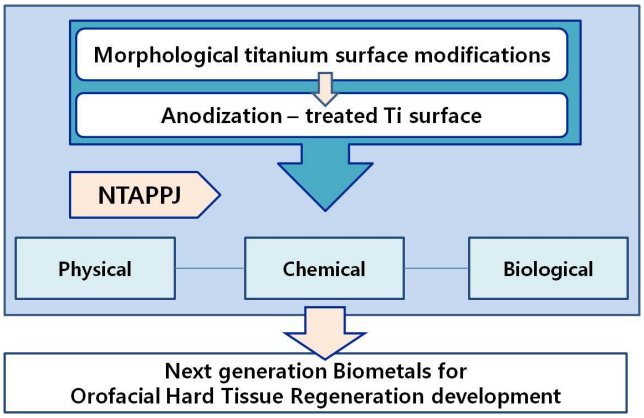

Figure 4. The schematic diagram of experimental group.

II. Materials and Methods

1. Preparation of TiO_2 nanotubes

Commercially pure Ti discs (grade IV, 10 x 10 x 0.4 mm) were polished with #400, #600, #800, #1200 and #2000 grit SiC sandpaper and were then ultrasonically cleaned with acetone, alcohol and distilled water, for 15 min each. The TiO_2 nanotubes were formed by electrochemical anodization using a direct current power supply (Genesys, 600-2.6 Densei-Lambda Tokyo, Japan), during which a constant voltage of 20 V was applied for 1 h with an electrolyte solution containing 0.1 wt% hydrofluoric acid (HF). The samples were then dried at room temperature during 24 h and annealed at 450 ºC. All the specimens were sterilized using ethylene oxide (EO) gas at a temperature of 55 ºC for 1 h before each experiment. EO gas sterilization was chosen for sterilization of TiO_2 nanotubes in the cell experiments because previous experiments we have verified that it has no effect on cell activity (Lee, 2013; Uhm , 2014).

2. Non-thermal atmospheric pressure plasma treatment

An NTAPPJ device was manufactured from the Plasma Bioscience Research Center (PBRC, Kwangwoon University, Korea); details concerning the device design can be found in a previous study (Ungvari, 2010). Briefly, the working gas (either compressed air or nitrogen) was used at a gas flow of 5 L/min, and the distance between the NTAPPJ tip and TiO_2 nanotube surface was set to 3 mm. Quartz with a depth of 3.2 mm was used as the dielectric and stainless steel was used as the outer electrode, which enclosed porous alumina of 150 to 200 μm pore size and 35% porosity. The total output power of the plasma was set to 2.4 W for both the nitrogen and air NTAPPJ. The discharges were formed at a discharge voltage of 2.24 kV and a discharge current of 1.08 mA. The discharge duration was 0.18 ms and the discharge filamentation frequency was 12 kHz during a discharge voltage period of 16 ms, which corresponds to a discharge frequency of 60 Hz. The number of discharges within the 1-ms discharge voltage period was approximately 100.

Three different NTAPPJ treatment times (0, 2 and 10 min) were used for the experiments. The groups subjected to these treatment times were labeled as NP0, NP2 and NP10 for nitrogen gas and as AP0, AP2 and AP10 for compressed air. NP0 and AP0 were used as controls.

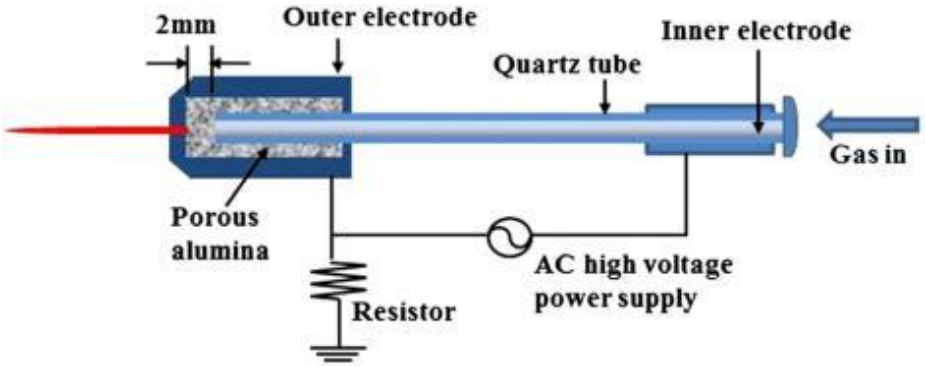

Figure 5. The schematic diagram of non-thermal atmospheric pressure plasma jet designed and manufactured by PBRC (Plasma Bioscience Research Center, Kwangwoon University, Korea, Choi, *et al*., 2013).

3. Surface Characterization

3.1. Field-emission scanning electron microscope (FE-SEM)

The morphologies of the TiO_2 nanotube surfaces before and after the 10 min NTAPPJ treatment were examined using a field-emission scanning electron microscope (FE-SEM, JSM-7100F, JEOL, Japan).

3.2. 3D surface profilometer

An optical profiler is device (Contour GT, Bruker, USA) that measures the surface height optically and represents the height as a color on a scale ranging from red to blue, on either 2D or 3D images of the surface. The optical profilometer was thus easily used for evaluation of the surface roughness difference at a particular position before and after treatment. The surface roughness characteristics were analyzed using the vertical scanning interferometry mode (VSI) using a green luminous source. Quantification of the roughness parameters was performed using software at a magnification of 10 X with a scanning area of 63 μm X 47 μm.

3.3. Contact angle measurements

The wettability of both the experiment and control samples was measured by dropping 4 μL of distilled water on the sample and then measuring the contact angle after 10 s using a video contact angle goniometer (Phoenix 300, SEO, Korea).

3.4. X-ray photoelectron spectroscopy (XPS)

The chemical compositions of the experiment and control sample surfaces were determined using an X-ray photoelectron spectroscope (XPS, K-alpha, Thermo VG, UK). Photoelectrons were generated by a monochromatic Al Kα line (1486.6 eV) X-ray source, and the beam was powered at 12 kV and 3 mA, at a beam diameter of 400 μm. The Ti2p, O1s, C1s and N1s peaks were analyzed for chemical property changes. The binding energy was calibrated using the C1s at the 284.8 eV peak.

4. Cellular activity

4.1. Cell Culture

A well-established cell lines of mouse fibroblast L929 (Korea Cell Line Bank, Seoul, Korea) was used for cell cytotoxicity test. Cells are RPMI (1640, Welgene, Korea) medium to 10% (W/V) fetal bovine serum (FBS, PAA Laboratoris.inc, A15-751) and 1% Penicillin (Lonza, walkersille MD, USA 0719) were mixed to 5% CO_2 and cultured at 37 ℃ incubator is supplied. The MC3T3-E1 murine pre-osteoblast cell line (CRL-2593, American Type Culture Collection, USA) was used for the cell attachment/viability test. The cells were cultured in alpha-MEM cell culture medium (LM008-01, Welgene, Korea) combined with 10 % fetal bovine serum (FBS, Gibco, USA), penicillin (100 units/ml, Gibco, USA) and streptomycin (100 mg/ml, Gibco, USA) at 37 °C in 5 % CO_2. The cell culture media were changed every 48 h. For the gene expression analysis test, rat mesenchymal stem cells (rMSC, Lonza, USA) were used. The cells were cultured in alpha-MEM supplemented with 10 % FBS and the same amount of penicillin/streptomycin as above. Cells from passages 3 to 5 were used in this study.

4.2. Cytotoxicity test

The cytotoxic evaluation of the non-thermal atmospheric pressure plasma treatment before / after the specimen was carried out on the basis of ISO 10993-5 and 10993-12. By setting the temperature and time control and experimental groups were used as solvents not only put the specimen. The water soluble tetrazolium (WST, Ez-Cytox, Daeillab, Korea) were tested using.

1 x 10^4 cells of L929 (100 ㎕) were placed on 96well plate and incubated under a constant humidified condition of 5% CO_2 at 37 ℃ for 24 hours. And eluate was reacted again in incubator for 24 hours. Assay reagent 10 ㎕ by dividing the each well and incubation was 4 hours.

The absorbance was then measured at 450 nm using ELISA reader (Epoch, Biotek Instruments Inc., Winooski, Vermont, U.S.A.).

4.3. Cell attachment and viability

For the cell attachment and viability experiment, 1 x 10^5 cells of MC3T3-E1 were placed on each of the test and control samples; after 4 h for attachment, the surfaces of the samples were washed using Dulbecco's phosphate-buffered saline (DPBS, Gibco, USA) to remove any non-adherent cells. Calcein AM and ethidium homodimer-1 stains (LIVE/DEAD Viability /Cytotoxicity Kit^{TM}, Invitrogen Co., Eugene, Oregon, USA) were then applied on each sample, and the levels of staining were assessed using a confocal laser microscope (CLSM 700, Carl Zeiss, Jena, Germany) to evaluate cell attachment and cell viability.

4.4. Cell proliferation

The numbers of cells (1 x 10^5 cells of MC3T3-E1) proliferation to the experiment and control surfaces were also assessed by water soluble tetrazolium (WST, Dae-il Lab, Seoul, Korea) assay. This assay was performed after 4 h, 24 h, 48h, 3 d and 5 d of culture, and the results are expressed as the percentage to the control sample. The absorbance was then measured at 450 nm using ELISA reader (Epoch, Biotek Instruments Inc., Winooski, Vermont, U.S.A.).

4.5. Cell differentiation: Gene expression analysis

Real-time reverse transcriptase-polymerase chain reaction (RT-PCR) was used to determine the mRNA expression levels of osteogenic genes for rMSCs cultured on the NTAPPJ-treated and NTAPPJ-untreated specimens. RT-PCR was used to analyze, in particular, the expression levels of alkaline phosphatase activity (ALP), runt-related transcription factor 2 (Runx2), osteopontin (OPN), osteocalcin (OCN) and the house-keeping gene glyceraldehyde 3-phosphate dehydrogenase (GAPDH). Following plasma treatment, 1 x 10^4 rMSCs were placed on both the control and experiment samples and were incubated at 37 °C in 5 % CO_2 for either 7 or 14 days. The total RNA was then isolated from the cells with Trizol reagent (Sigma-Aldrich Company, St. Louis, MO, USA), and the RNA was converted into cDNA using an Omniscript® RT kit (Qiagen, Hilden, Germany), which was incubated at 37 °C for 90 min. Data analysis was performed using an ABI Prism 7500 machine (Applied Biosystems, Foster City, CA, USA). The conditions for PCR were as follows: a 95 ºC/10 minute activation step, followed by a denaturation step of 95 °C/15 seconds and a primer extension of 60 °C/minute for 40 cycles. The gene expression data were normalized with GAPDH expression, and the results are expressed as the relative fold increase in gene expression compared with the control, i.e. TiO_2 nanotubes not treated with NTAPPJ.

Table 2. Primer sequences for the gene observed in this study

Gene	Primer sequences
GAPDH	(F) GAA OCT GOC GTG GGT AGA G
	(R) AGG TOG GTG TGA AOG GAT TTG
ALP	(F) AGG CAG GAT TGA CCA CGG
	(R) TGT AGT TCT GCT CAT GGA
OCN	(F) CAG OOC CCT ACC CAG AT
	(R) TGT GOC GTC CAT ACT TTC
OPN	(F) CAA GGT TGC AGA CAC TGA AAG
	(R) CAT TTC TAG AAG GGT GAC AGG
Runx-2	(F) AGC AAC AGC AAC AAC AGC AG
	(R) GTA ATC TGA CTC TGT CCT TG

(F); Forward sequences, (R); Reverse sequences, GAPDH; glyceraldehyde 3-phosphate dehydrogenase, ALP; Alkaline phosphates, OCN; osteocalcin, OPN; osteopontin, Runx-2; runt-related transcription factor 2.

5. Statistical analysis

All of the cellular experiments were performed 3 times using 4 samples of each experiment and control group. To identify any significant differences between the groups, the data were subjected to independent t-test, one-way analysis of variance (ANOVA) test and ^{abc}denotes the same subgroup by Tukey post-hoc analysis. Significance was determined at the 95 % confidence level.

III. RESULTS

1. Surface analysis

1.1. Field-emission scanning electron microscope (FE-SEM)

Figure 6 presents FE-SEM images of the morphology of the TiO_2 nanotube surface before (Figure 6A) and after (Figures 6B and C). The results indicate that there was no change in the topographic characteristics of the TiO_2 nanotube surfaces in morphology.

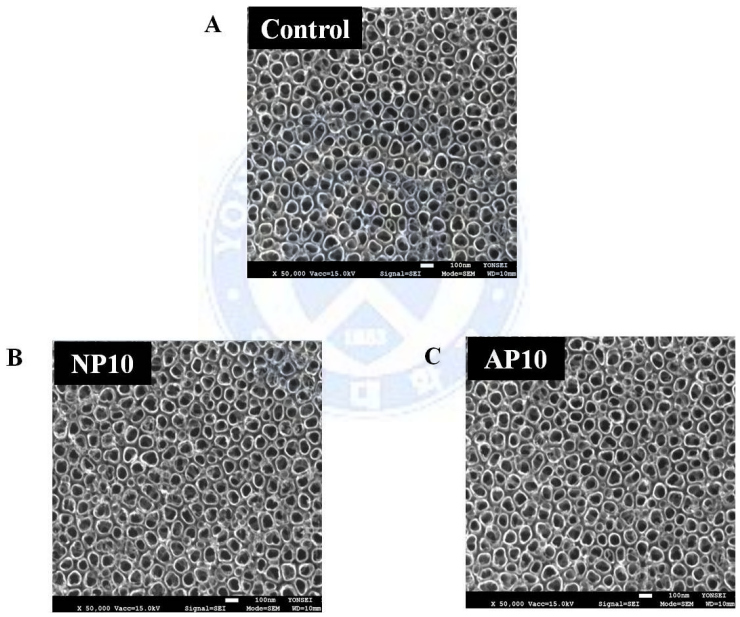

Figure 6. FE-SEM micrographs of the Ti specimens of the TiO_2 nanotubes.

A: untreated TiO_2 nanotubes (control), B: TiO_2 nanotubes with 10-min nitrogen-based NTAPPJ treatment, C: TiO_2 nanotubes with 10-min air-based NTAPPJ treatment. Scale Bar: 100 μm.

1.2. 3D surface profilometer

The result of the average surface roughness (Ra) values with NTAPPJ treatment determined using a surface profiler (Figure 7). The results indicate that there was no significant of the TiO_2 nanotube surfaces in average roughness values ($P > 0.05$).

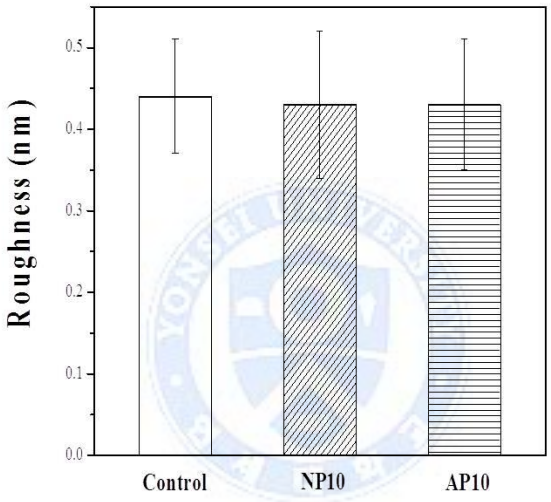

Figure 7. Shows the average surface roughness (Ra) values determined using a surface profiler. control: untreated TiO_2 nanotubes, NP10: TiO_2 nanotubes with 10-min nitrogen-based NTAPPJ treatment, AP10: TiO_2 nanotubes with 10-min air-based NTAPPJ treatment.

1.3. Contact angle measurement

The contact angle measurements are listed in terms of either Figure 8 or Table 3. The water contact angle of the TiO_2 nanotube surface was significantly reduced following NTAPPJ treatment ($P<0.05$), where both the NP2 and NP10 group are observed to be ultra-hydrophilic with contact angles of 0º. However, despite the significant decrease in contact angles for the AP2 and AP10 groups, their contact angles were reduced less compared with the control group than NP2 and NP10.

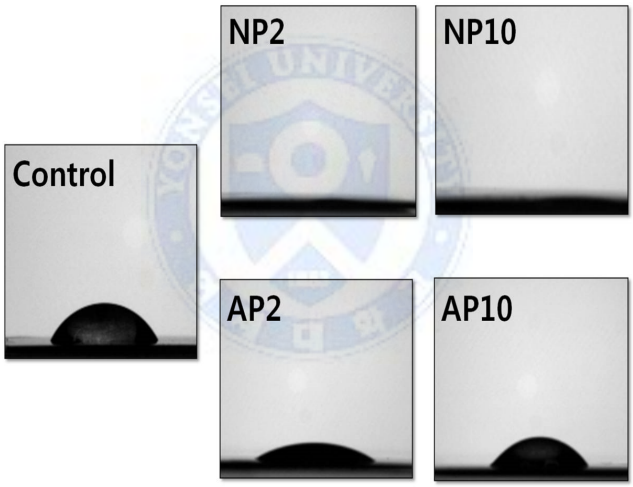

Figure 8. Contact angle of control and experimental groups measured.

NP0 and AP0: untreated TiO_2 nanotubes with no treatment (control group); NP2: TiO_2 nanotubes with 2-min nitrogen-based NTAPPJ; NP10: TiO_2 nanotubes with 10-min nitrogen-based NTAPPJ; AP2: TiO_2 nanotubes with 2-min air-based NTAPPJ; AP10: TiO_2 nanotubes with 10-min air-based NTAPPJ.

Table 3. The water contact angle (º) of the control and test TiO_2 nanotube surfaces at room temperature.

Samples	**Contact angle (º) (Mean ± standard deviation)**
Control group	46.4 ± 4.0^{a}
NP2	0.0^{b*}
NP10	0.0^{b*}
AP2	$26.38 \pm 4.43^{c*}$
AP10	$33.81 \pm 5.10^{c*}$

NP2: TiO_2 nanotube with 2-min nitrogen-based NTAPPJ; NP10: TiO_2 nanotube with 10-min nitrogen-based NTAPPJ; AP2: TiO_2 nanotube with 2-min air-based NTAPPJ; AP10: TiO_2 nanotube with 10-min air-based NTAPPJ. The symbol '*' indicates a significant difference compared with the control group when analyzed using one-way ANOVA and ^{abc}denotes the same subgroup by Tukey post-hoc analysis ($p<0.05$).

1.4.XPS

1.4.1. The XPS spectra

The XPS spectra revealed peaks of Ti2p, O1s, C1s and N1s Figures 9A to H, I and II. A Ti2p doublet peak is visible, containing both Ti2p 1/2 and Ti2p 3/2 components and appearing at 464.3 eV to 458.7 eV (difference of Δ5.6 eV).

The O1s spectra, presented in Figures 9C and D, contain a peak corresponding to TiO_2 near 530.0 eV; the presence of this peak was attributed to the lattice oxygen in the sample (Ungvari, 2010). And a peak at 532.4 eV to 530.7 eV corresponding to the hydroxyl groups (O-H) (Moulder, 1992; Hyam, 2012).

In addition, the peak at 532.9 eV is associated with C-O and/or C=O bonds (Ungvari, 2010). The Ti2p and O1s peaks were slightly shifted to higher binding energies in the experimental groups compared with the control group.

In terms of the C1s peaks (Figures 9E and F), the peak corresponding to hydrocarbon (284.7 eV) decreased in the experimental groups. Additionally, the shoulder peak between 290.5 eV and 288.0 eV (O-C=O) significantly shifted to a higher binding energy for all of the experimental groups compared with the control group (Yamamoto, 2005; Aita, 2009). And there are peak of COOH indicating at 288.9 eV.

The peak of NH_2, NH, NH_3+ (Figures 9G and H) was located at 399.6

eV, 400.4 eV, 401.7 eV, respectively (Yamamoto, 2005; Lee 2014). The peak of N1s in the XPS corresponds to the NH^+ groups of amino groups (Feng *et al.,* 2004). The experimental groups were an increase in peak shift high intensity compared with the control group.

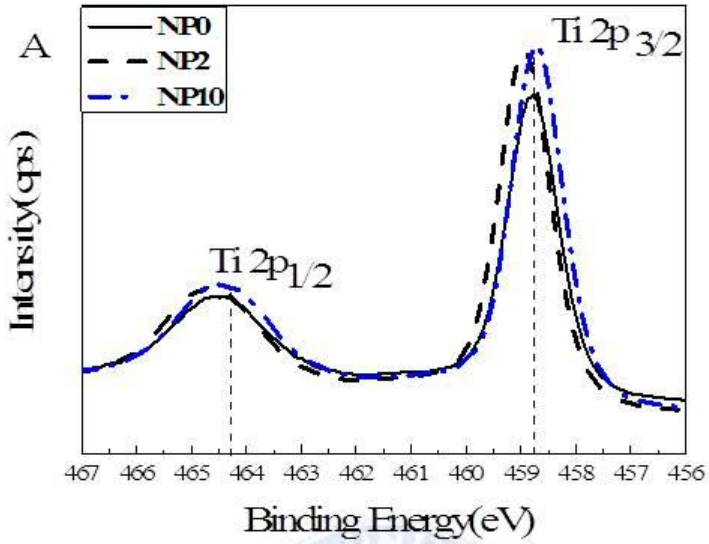
A
NP0
NP2
NP10
Ti 2p 3/2
Ti 2p1/2
Intensity(cps)
467 466 465 464 463 462 461 460 459 458 457 456
Binding Energy(eV)

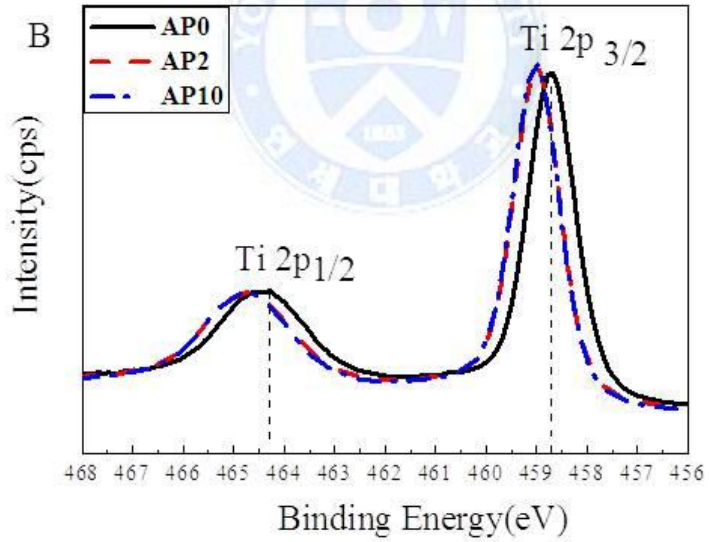
B
AP0
AP2
AP10
Ti 2p 3/2
Ti 2p1/2
Intensity(cps)
468 467 466 465 464 463 462 461 460 459 458 457 456
Binding Energy(eV)

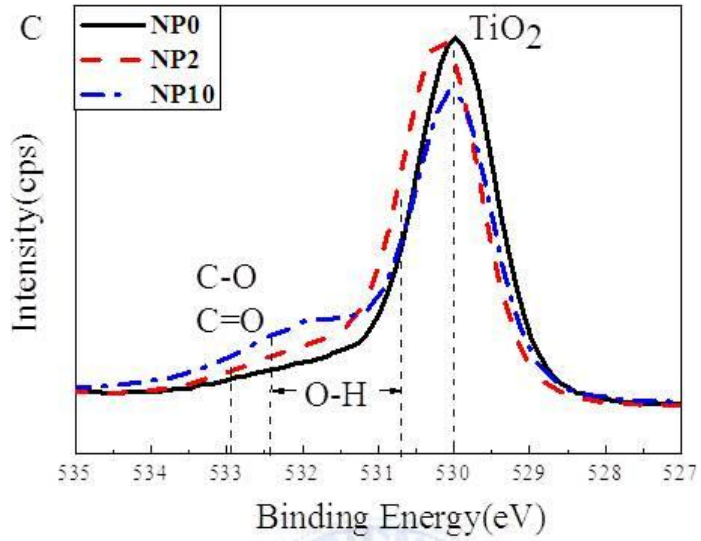
C
NP0
NP2
NP10
TiO2
Intensity(cps)
C-O
C=O
O-H
535
534
533
532
531
530
529
528
527
Binding Energy(eV)

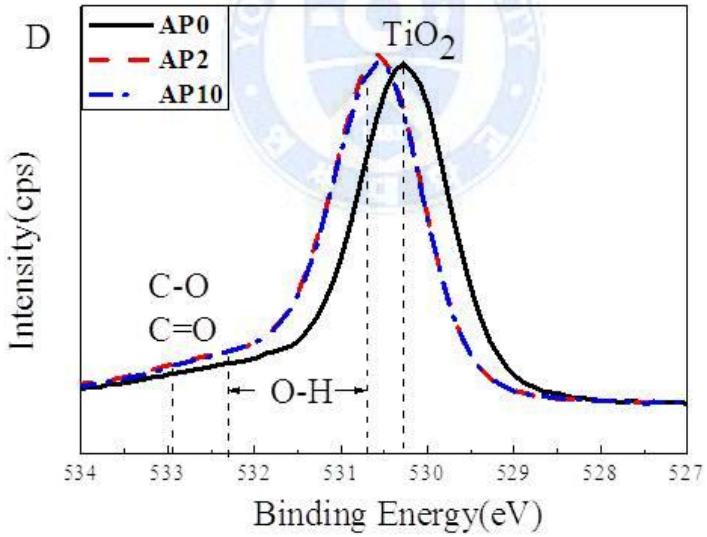
D
AP0
AP2
AP10
TiO2
Intensity(cps)
C-O
C=O
O-H
534
533
532
531
530
529
528
527
Binding Energy(eV)

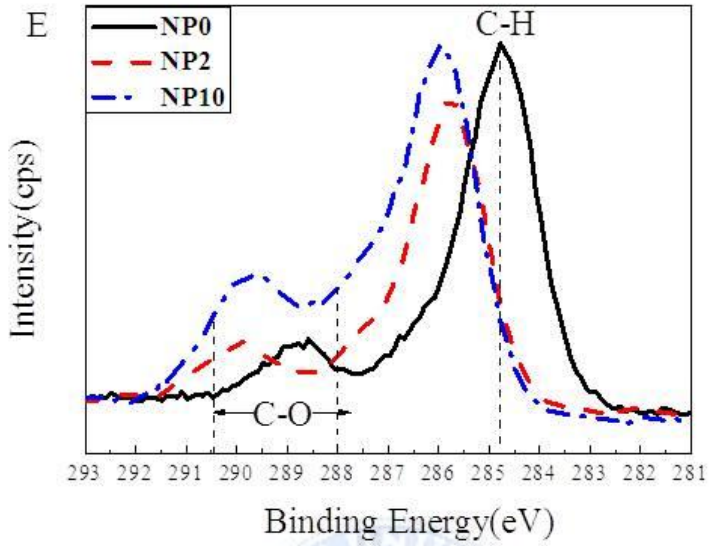
E
NP0
NP2
NP10
C-H
C-O
Intensity(cps)
293 292 291 290 289 288 287 286 285 284 283 282 281
Binding Energy(eV)

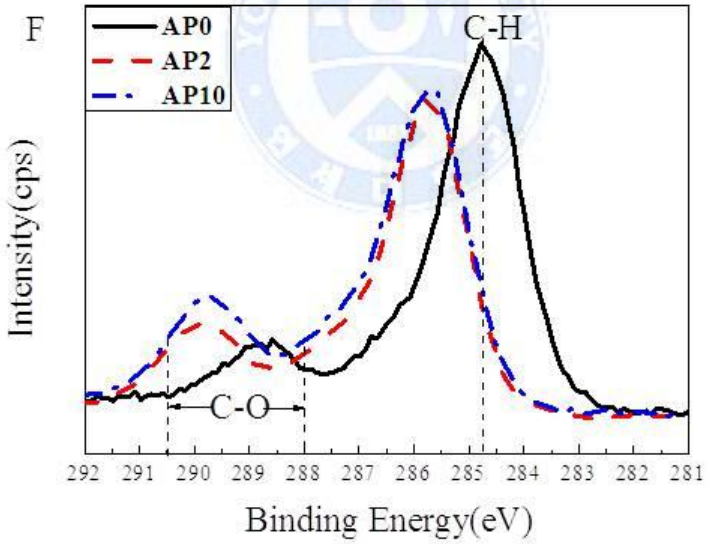
F
AP0
AP2
AP10
C-H
C-O
Intensity(cps)
292 291 290 289 288 287 286 285 284 283 282 281
Binding Energy(eV)

G

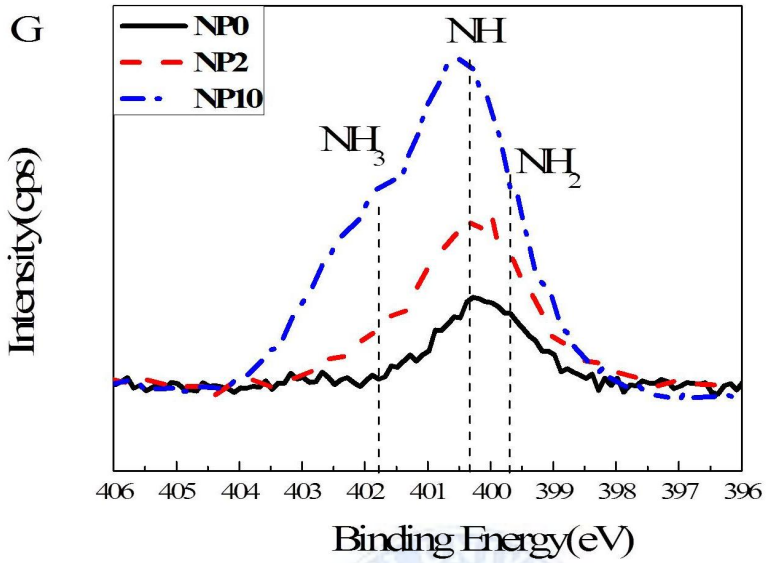
NP0
NP2
NP10
NH
NH3
NH2
Intensity(cps)
406 405 404 403 402 401 400 399 398 397 396
Binding Energy(eV)

H

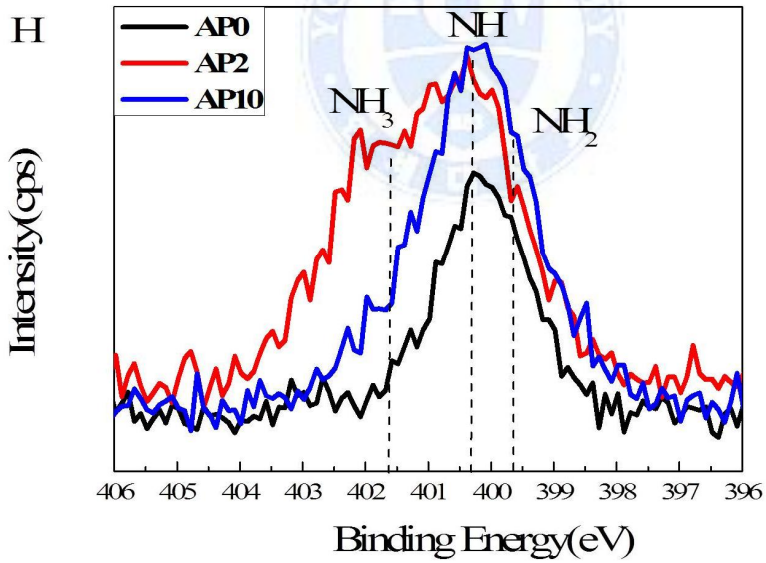
AP0
AP2
AP10
NH
NH3
NH2
Intensity(cps)
406 405 404 403 402 401 400 399 398 397 396
Binding Energy(eV)

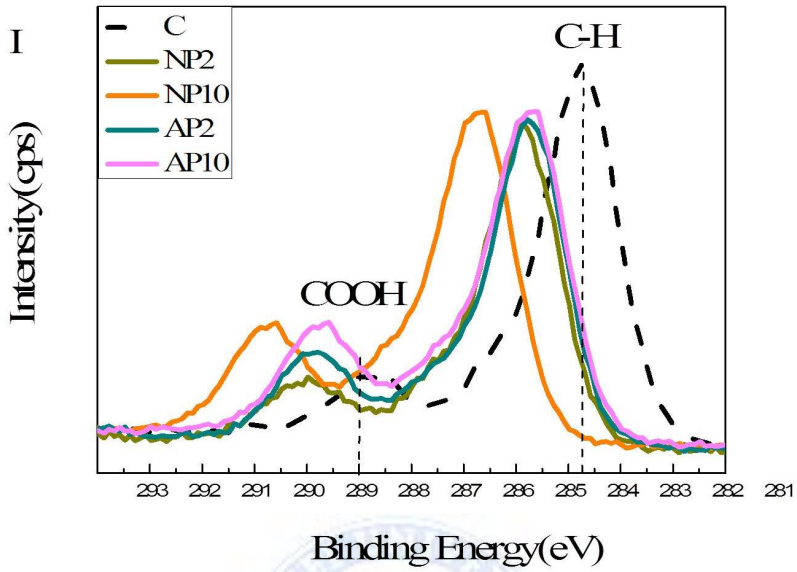
I
C
NP2
NP10
AP2
AP10
C-H
COOH
Intensity(cps)
293 292 291 290 289 288 287 286 285 284 283 282 281
Binding Energy(eV)

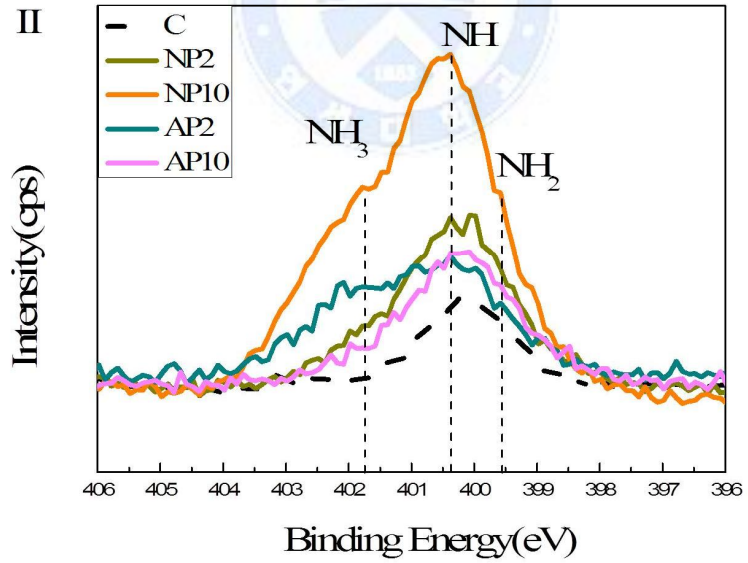
II
C
NP2
NP10
AP2
AP10
NH
NH3
NH2
Intensity(cps)
406 405 404 403 402 401 400 399 398 397 396
Binding Energy(eV)

Figure 9. Chemical composition of a TiO_2 nanotube surface measured with XPS. A, B / Ti2p spectra; C, D / O1s spectra; E, F / C1s spectra and G, H / N1s spectra.

NP0 and AP0: untreated TiO_2 nanotubes with no treatment (control group); NP2: TiO_2 nanotubes with 2-min nitrogen-based NTAPPJ; NP10: TiO_2 nanotubes with 10-min nitrogen-based NTAPPJ; AP2: TiO_2 nanotubes with 2-min air-based NTAPPJ; AP10: TiO_2 nanotubes with 10-min air-based NTAPPJ.

1.4.2. The atomic percentage of XPS

The atomic percentage of each element was analyzed from the XPS peaks Figure 10. The carbon contents in the experimental groups were lower than that of the control group (19.0 %). The nitrogen-based NTAPPJ treatment group (NP2 15.9 %, NP10 13.5 %) exhibited a lower carbon content than the air-based NTAPPJ treatment group (AP2 16.5 %, AP10 17.9%) for the same duration of exposure.

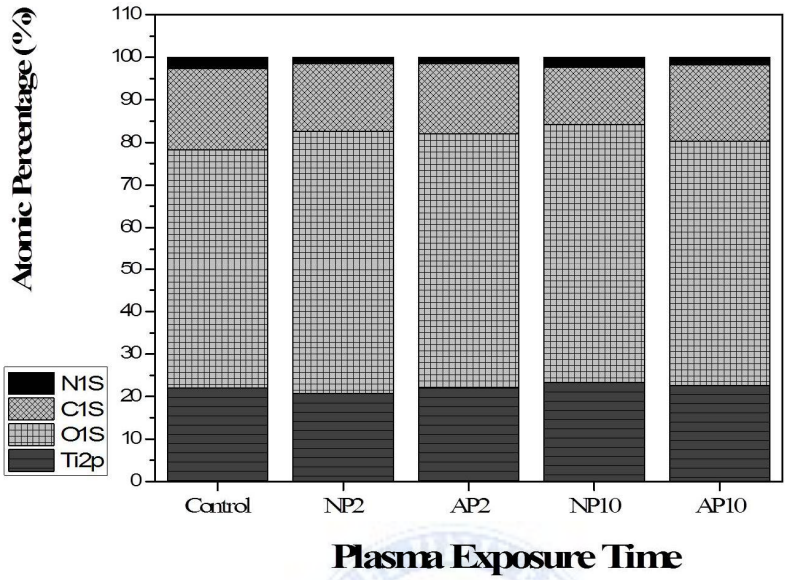

Figure 10. Atomic percentage of each element on the surface of TiO_2 nanotubes before and after nitrogen- or air-based NTAPPJ treatment.

NP2: TiO_2 nanotubes with 2-min nitrogen-based NTAPPJ; NP10: TiO_2 nanotubes with 10-min nitrogen-based NTAPPJ; AP2: TiO_2 nanotubes with 2-min air-based NTAPPJ; AP10: TiO_2 nanotubes with 10-min air-based NTAPPJ.

2. Cellular activity

2.1. Cytotoxicity test

The NTAPPJ treatment were examined for effects on cytotoxicity. If there is more than 80% cell viability was determined that there is no cell toxicity. As a result, no cytotoxicity was found to be in all the specimens, nitrogen NTAPPJ examined for cell viability was higher than the air NTAPPJ treatments (Figure 11).

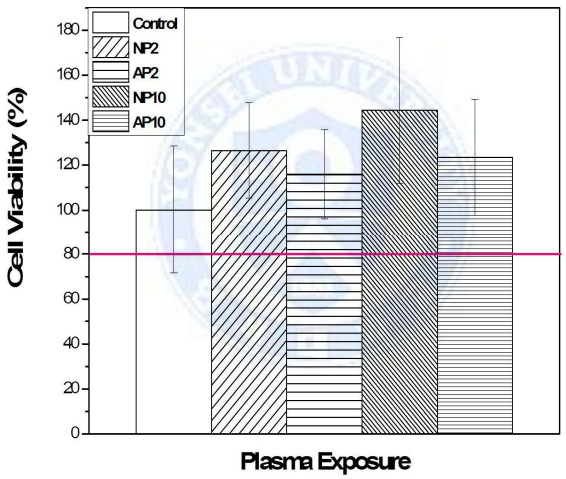

Figure 11. The viability of L929 cells tested. Control: untreated TiO_2 nanotubes with no treatment; NP2: TiO_2 nanotubes with 2-min nitrogen-based NTAPPJ; NP10: TiO_2 nanotubes with 10-min nitrogen-based NTAPPJ; AP2: TiO_2 nanotubes with 2-min air-based NTAPPJ; AP10: TiO_2 nanotubes with 10-min air-based NTAPPJ.

2.2. Morphology of attached cell

: confocal laser microscope analysis

The cells were stained with calcein AM and ethidium homodimer-1 to determine both the number of cells attached to a sample and the viability of the cells, as indicated by the green (live cells) or red (dead cells) colors in images (Figure 12). The smallest numbers of cells were attached to the substrates in the control group, and some cells appeared to be dead on these samples. In contrast, all of the cells on the test samples were green (indicating live cells), and a relatively large number of cells were attached. Additionally, the cells were rounder in shape for the control group, whereas cells had stretched shapes in the experimental group. In particular, the cells on NP2 and NP10 contained more stretched filopodia than the cells in the control groups, AP2 and AP10.

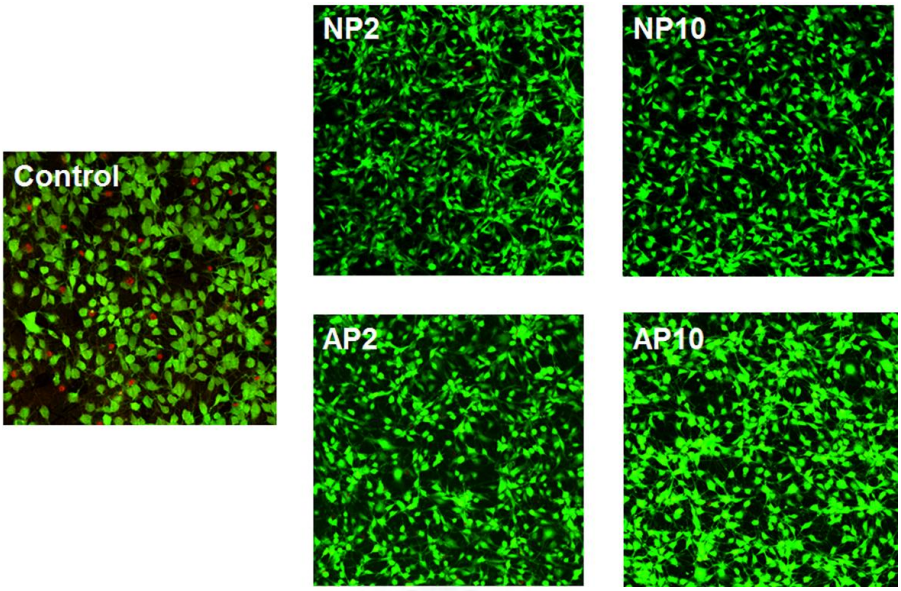

Figure 12. Cell attachment and viability on TiO_2 nanotubes before and after the NTAPPJ treatment. Live cells are green, and dead cells are red. Control: untreated TiO_2 nanotubes with no treatment; NP2: TiO_2 nanotubes with 2-min nitrogen-based NTAPPJ; NP10: TiO_2 nanotubes with 10-min nitrogen-based NTAPPJ; AP2: TiO_2 nanotubes with 2-min air-based NTAPPJ; AP10: TiO_2 nanotubes with 10-min air-based NTAPPJ.

2.3. Cell proliferation

The numbers of cells attachment and proliferation to each of the control and test samples are presented in Figure 13 (a) and (b). From these results, it is apparent that there was significant increase compared with control group ($p<0.05$). In the numbers of attached cells following exposure to either air or nitrogen-based NTAPPJ compared to the control group, for any exposure time. Furthermore, in both days 3 and 5 of cell culture, there was a significant difference in the numbers of cells that proliferated onto samples treated with air-based NTAPPJ and those that proliferated onto samples treated with nitrogen-based NTAPPJ for each of duration of exposure. In all cases, nitrogen-based NTAPPJ-treated TiO_2 nanotubes displayed better cell proliferation ($p<0.05$).

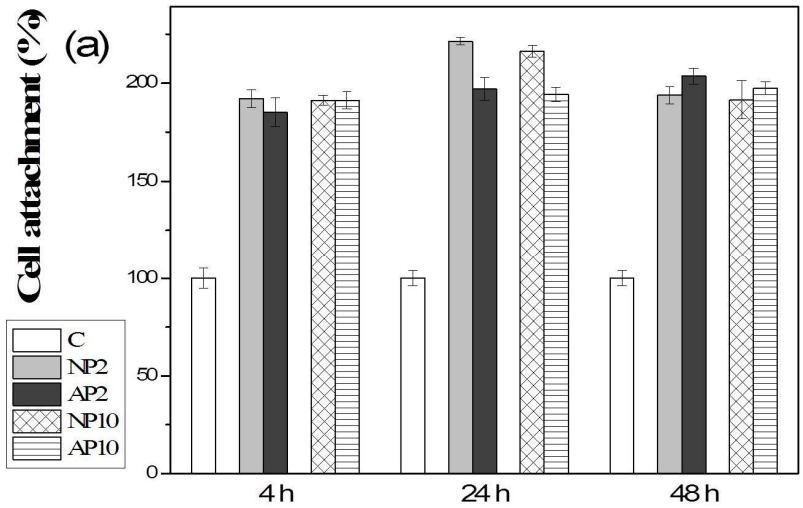
(a)
Cell attachment (%)
200
150
100
50
0
C
NP2
AP2
NP10
AP10
4 h
24 h
48 h

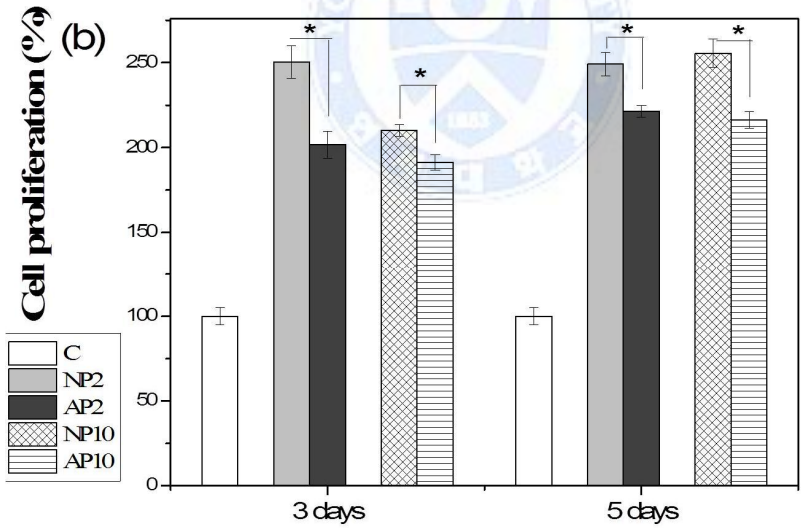
(b)
Cell proliferation (%)
250
200
150
100
50
0
*
*
*
*
C
NP2
AP2
NP10
AP10
3 days
5 days

Figure 13. Numbers of cells attachments (a) and proliferation (b) on the surface of TiO_2 nanotubes before and after the NTAPPJ treatment. C: untreated TiO_2 nanotubes with no treatment; NP2: TiO_2 nanotubes with 2-min nitrogen-based NTAPPJ; NP10: TiO_2 nanotubes with 10-min nitrogen-based NTAPPJ; AP2: TiO_2 nanotubes with 2-min air-based NTAPPJ; AP10: TiO_2 nanotubes with 10-min air-based NTAPPJ. Significant differences in numbers of cell attachments between NTAPPJ with different gas sources for the same duration of exposure on TiO_2 nanotubes are marked with '*' ($p<0.05$).

2.4. Cell differentiation : gene expression analysis

The gene expression of the specimens was measured by RT-PCR at 7 and 14 days post-irradiation. Figure 14 shows the gene expression of ALP, Runx2, OCN and OPN. In general, the gene expression of ALP, Runx2, OCN and OPN in the NP2, NP10, AP2 and AP10 groups was higher than that of the control group ($p<0.05$). When comparing the effects of treatment with either nitrogen- or air-based gas on gene expression at 14 days after the same radiation dose, the nitrogen-based NTAPPJ treatment was observed to induce a higher level of gene expression than the air-based NTAPPJ treatment for a 2-min exposure time, except in the case of OCN expression ($p<0.05$).

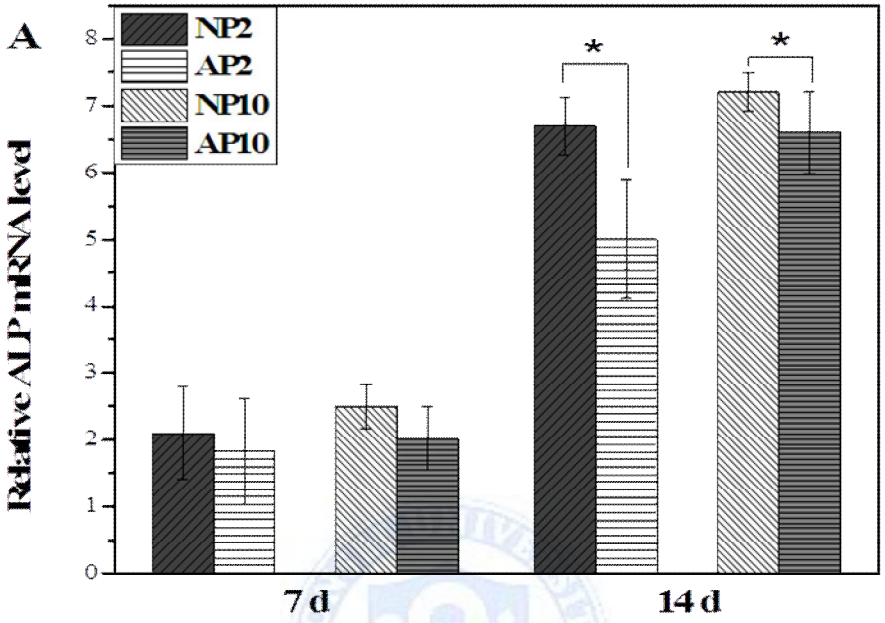
A
NP2
AP2
NP10
AP10
Relative ALP mRNA level
0
1
2
3
4
5
6
7
8
*
*
7 d
14 d

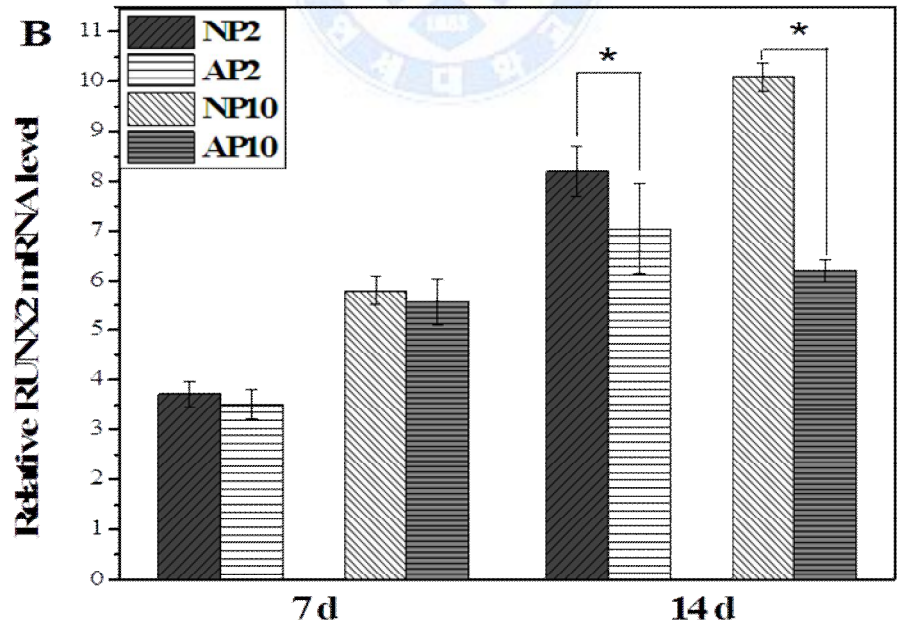
B
NP2
AP2
NP10
AP10
Relative RUNX2 mRNA level
0
1
2
3
4
5
6
7
8
9
10
11
*
*
7 d
14 d

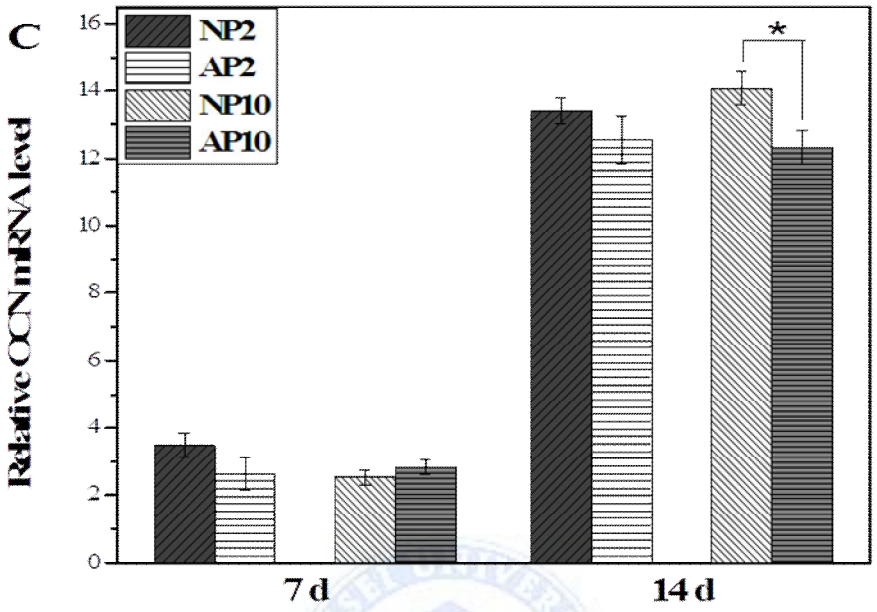
C
Relative OCN mRNA level
NP2
AP2
NP10
AP10
16
14
12
10
8
6
4
2
0
*
7 d
14 d

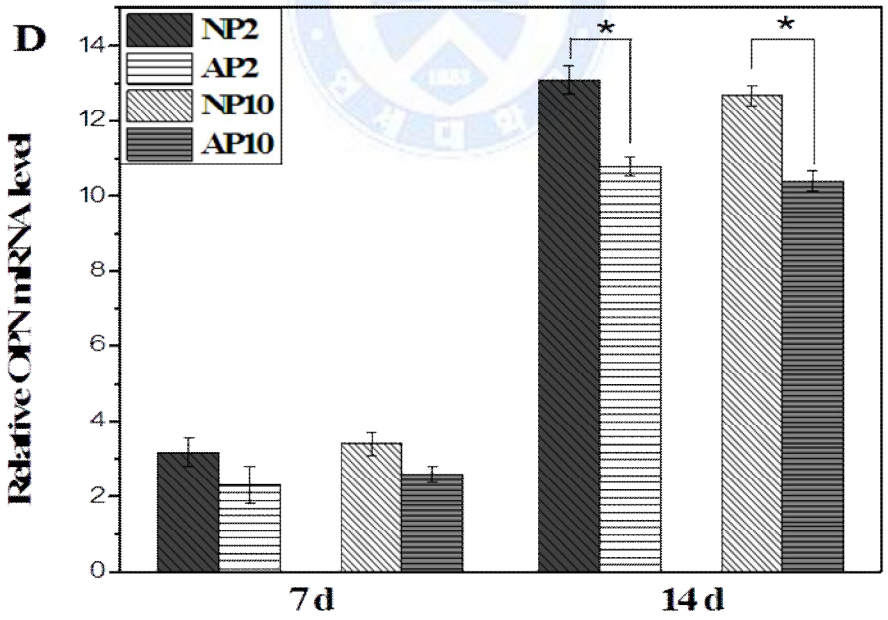
D
Relative OPN mRNA level
NP2
AP2
NP10
AP10
14
12
10
8
6
4
2
0
*
*
7 d
14 d

Figure 14. Real-time PCR results for relative osteogenic gene expression of rMSCs cultured on TiO_2 nanotubes for 7 and 14 days. Significant differences in relative gene expression between NTAPPJ with different gas sources for the same duration of exposure on TiO_2 nanotubes are marked with '*' ($p< 0.05$).

Control: untreated TiO_2 nanotubes; NP2: TiO_2 nanotubes with 2-min nitrogen-based NTAPPJ; NP10: TiO_2 nanotubes with 10-min nitrogen-based NTAPPJ; AP2: TiO_2 nanotubes with 2-min air-based NTAPPJ; AP10: TiO_2 nanotubes with 10-min air-based NTAPPJ.

IV. Discussion

The osseointegration of an implant is determined by the features of the implant surface, where the preservation of them through avoiding the material aging effects is important. The aim of this study was to apply the recently highlighted portable NTAPPJ on TiO_2 nanotubes to improve their hydrophilicity and osteogenic properties while preserving the morphology of the nanotubular structure from the anodization procedure and avoiding the aging effects through portability.

The results of the morphological and topographical analysis before and after NTAPPJ treatment revealed that NTAPPJ treatment has no effect on the TiO_2 nanotubular morphology (Figure 6), or average roughness value (Figure 7), which is consistent with previous studies that applied NTAPPJ on the surfaces of other biomaterials (Kalghatgi, 2011; Choi, 2013).

Despite the preservation of the morphology and topography, the hydrophilicity was significantly different between the untreated TiO_2 nanotube surface and that treated with NTAPPJ. The distilled water contact angle of the TiO_2 nanotube surface with the nitrogen- and air-based NTAPPJ treatment was significantly lower than that of the control group (Figure 8 and Table 3, $P<0.05$). This improvement of hydrophilicity is expected to contribute to the osteogenicity of TiO_2 nanotubes (He, 2008). Notably, the NP2 and NP10 groups resulted in contact angles of zero degrees, whereas the

contact angles of the AP2 and AP10 groups were less changed from the control.

These changes were accompanied by the carbon composition of the samples before and after the NTAPPJ treatment as determined by XPS analysis (Figure 10), which affected cell morphology (Figure 12), attachment (Figure 13 (a)), proliferation (Figure 13 (b)) and cell gene expression (Figure 14).

The removal of carbohydrates in the link to the C-H peak is known to induce an increased surface energy of the biomaterial surface, resulting in an increased hydrophilic state (Choi, 2013). Additionally, it is well known that carbon induces the worst effects on cell viability (Malkoc, 2012), and the reduction of carbon percentage on the surface of biomaterials is known to result in increased cellular attachment and the promotion of osteoblastic differentiation during implantation (Aita, 2009; Walter, 2013). In this study, the atomic percentage of each element analyzed from the XPS peaks (Figure 10) indicated that the carbon content in the experimental group was reduced after the NTAPPJ treatment. The XPS results showed increased O-H, COOH, NH, NH_2, on the surfaces of the NTAPPJ-treated TiO_2 nanotubes compared with the controls. Additionally, the C-H and C–C peaks decreased after the nitrogen- and air-based NTAPPJ treatments, whereas the O1s and TiO_2 peaks increased (Figure 9). Previous study, increase in the O-H group triggers better osteoblast and increased mRNA levels of osteocalcin on titanium surfaces (Walter, 2013), and up-regulated osteoblast gene expression, ALP activity and

matrix mineralization (Keselowsky, 2005). The NH^+ groups of amino groups and attributable to adsorbed extracelluar matrix (ECM) proteins (Feng *et al*., 2004; Yamamoto 2005), NH_2 up-regulated osteoblast gene expression, ALP activity and matrix mineralization (Keselowsky, 2005) such as O-H. When the plasma treatment, chemical functional groups such as COOH, OH, NH_2 was promoting cell differentiation and osteoblast (Lee, 2014).

This result indicates that the constituents of plasma are energetic enough to break the C-C and C-H bonds at the surface layer to form radicals that yield various oxygen functionalities on the surface via subsequent oxidation chemistry. The resultant reduction in the carbon content of the TiO_2 nanotube surface resulted in higher levels of hydrophilicity (Figure 9), cell attachment and viability of cells (Figure 12) on the NTAPPJ-treated specimens compared with the controls.

The EO gas sterilization was used as the method of sterilization for all of samples in this study as it is commonly used for the medical and dental devices. However, previous studies indicated that the cell attachment levels were lower with the EO gas treated samples though there was no correlation with numbers of sterilization cycles (Vezeau, 1996; Thierry, 2000). Hence, the results of reduced cell attachment for untreated TiO_2 nanotube surface in our study may have been affected by EO gas sterilization. Having said that, our previous studies with same method of sterilization, EO gas (Lee, 2013; Uhm, 2014), have shown that there was no indication of compromised cellular

attachment on the sterilized samples and therefore, the effects seen here is not solely by the method of sterilization. Additionally, in terms of the gas supply of NTAPPJ, the nitrogen-based NTAPPJ treatment group exhibited lower carbon content than the air-based NTAPPJ treatment group for the same duration of exposure (Figure 10). This finding is correlated with the results of RT-PCR at 14 days of rMSC culture, which indicated that the nitrogen-based NTAPPJ treatment induced higher osteogenic gene expression than the air-based NTAPPJ treatment (Kwon, 2006; Walter, 2013).

In general, an enhancing osseointegration capacity was demonstrated for both the nitrogen- and air-based NTAPPJ treatment, and the application of this technology is expected to be extendable to other surface types that comprise most of the currently available Ti implants (Aita, 2009).

V. Conclusion

In conclusion, nitrogen- and air-based NTAPPJ treatment on TiO_2 nanotube surfaces is effective in increasing the hydrophilicity and osseointegration of dental implants compared to the control group. However, the nitrogen-based NTAPPJ treatment group resulted in a higher osteogenic gene expression level accompanied by the atomic percentage of carbon decreasing more than that of the air-based NTAPPJ treatment group. Hence, nitrogen gas is recommended if one gas needs to be selected; however, the clinical gas of compressed air will be easier to obtain (with a built-in compressor available in most clinics).

The results of this study are limited to *in vitro* applications, and *in vivo* studies or studies of other implant surfaces may be needed to confirm the validity of these results. Despite these limitations, it is concluded that NTAPPJ treatment on TiO_2 nanotubes improved cellular attachment and differentiation without resulting in topographical changes.

REFERENCES

Aita H, Hori N, Takeuchi M, Suzuki T, Yamada M, Anpo M, et al. (2009). The effect of ultraviolet functionalization of titanium on integration with bone. *Biomaterials* 30(6): 1015-1025.

Albrektsson T, Wennerberg A (2005). The impact of oral implants - Past and future, 1966-2042. *J Can Dent Assoc* 71:327-327d.

Anselme K, Bigerelle M (2006). Effect of a gold-palladium coating on the long-term adhesion of human osteoblasts on biocompatible metallic materials. *Surf Coat Technol* 200(22-23): 6325-6330.

Chien C.C, Liu KT, Duh JG, Chang KW, Chung KH (2008). Effect of nitride film coatings on cell compatibility. *Dent Mater* 24(7): 986-993.

Choi YR, Kwon JS, Song DH, Choi EH, Lee YK, Kim KN, et al. (2013). Surface modification of biphasic calcium phosphate scaffolds by non-thermal atmospheric pressure nitrogen and air plasma treatment for improving osteoblast attachment and proliferation. *Thin Solid Films* 547: 235-240.

Duske K, Koban I, Kindel E, Schroder K, Nebe B, Holtfreter B, et al. (2012).

Atmospheric plasma enhances wettability and cell spreading on dental implant metals. *J Clin Periodontol* 39(4): 400-407.

Ellingsen JE, Johansson CB, Wennerberg A, Holmen A (2004). Improved retention and bone-tolmplant contact with fluoride-modified titanium implants. *Int J Oral Maxillofac Implants* 19(5): 659-666.

Faghihi S, Azari F, Li H, Bateni MR, Szpunar JA, Vali H, et al. (2006). The significance of crystallographic texture of titanium alloy substrates on pre-osteoblast responses. *Biomaterials* 27(19): 3532-3539.

Feng B, Weng J, Yang BC, Qu SX, Zhang XD (2004). Characterization of titanium surfaces with calcium and phosphate and osteoblast adhesion. *Biomaterials* 25(17): 3421-3428.

Fridman AA (2008). Inorganic gas-phase plasma decomposition processes. In: Plasma chemistry. AA Fridman editor. Cambridge: Cambridge University, pp. 259–355.

He J, Zhou W, Zhou X, Zhong X, Zhang X, Wan P, Zhu B, Chen W (2008). The anatase phase of nanotopography titania plays an important role on osteoblast cell morphology and proliferation. *J Mater Sci Mater Med* 19(11):

3465-3472.

Hyam RS, Lee J, Cho E, Khim J, Lee H (2012). Effect of annealing environments on self-organized TiO2 nanotubes for efficient photocatalytic applications. *J Nanosci Nanotechnol* 12(12): 8908-8912.

Ikeda D, Ogawa M, Hara Y, Nishimura Y, Odusanya O, Azuma K, et al. (2002). Effect of nitrogen plasma-based ion implantation on joint prosthetic material. *Surf Coat Technol* 156(1-3): 301-305.

Kaivosoja E, Barreto G, Levón K, Virtanen S, Ainola M, Konttinen Y (2012). Chemical and physical properties of regenerative medicine materials controlling stem cell fate. *Annals Med* 44(7): 635-650.

Kalghatgi S, Kelly CM, Cerchar E, Torabi B, Alekseev O, Fridman A, et al. (2011). Effects of non-thermal plasma on mammalian cells. *PLoS One* 6(1): e16270.

Kawai H, Shibata Y, Miyazaki T (2004). Glow discharge plasma pretreatment enhances osteoclast differentiation and survival on titanium plates. *Biomaterials* 25(10): 1805-1811.

Keselowsky BG. Collard DM, Garcia AJ(2005).Integrin binding specificity regulates biomaterial surface chemistry effects on cell differentiation *Proc Nalt Acad Sci USA* 102(17): 5953–5957.

Kim H, Murakami H, Chehroudi B, Textor M, Brunette DM (2006). Effects of surface topography on the connective tissue attachment to subcutaneous implants. *Int J Oral Maxillofac Implants* 21(3): 354-365.

Klokkevold PR, Nishimura RD, Adachi M, Caputo A (1997).Osseointegration enhanced by chemical etching of the titanium surface. A torque removal study in the rabbit. *Clin Oral Implants Res* 8(6): 442-447.

Kumar N, Attri P, Yadav DK, Choi J, Choi EH, Uhm HS (2014). Induced apoptosis in melanocytes cancer cell and oxidation in biomolecules through deuterium oxide generated from atmospheric pressure non-thermal plasma jet. *Sci Rep* 23(4): 7589.

Kwon OJ, Myung SW, Lee CS, Choi HS (2006). Comparison of the surface characteristics of polypropylene films treated by Ar and mixed gas (Ar/O2) atmospheric pressure plasma. *J Colloid Interface Sci* 295(2): 409-416.

Bardos L, Barankova H (2010). Cold atmospheric plasma: Sources, processes,

and applications. *Thin Solid Films* 518(23): 6705-6713.

Lavenus S, Louarn G, Layrolle P (2010). Nanotechnology and dental implants. *Int J Biomater* 2010: 915327.

Le Guehennec L, Soueidan A, Layrolle P, Amouriq Y (2007). Surface treatments of titanium dental implants for rapid osseointegration. *Dent Mater* 23(7): 844-854.

Lee EJ, Kwon JS, Om JY, Moon SK, Uhm SH, Choi EH, Kim KN (2014). The enhanced integrin-mediated cell attachment and osteogenic gene expression on atmospheric pressure plasma jet treated micro-structured titanium surfaces. *Curr Appl Phys* 14:S167- S171.

Lee JH, Ogawa T (2012). The biological aging of titanium implants. *Implant Dent* 21(5): 415-421.

Lee JH, Moon SK, Kim KM, Kim KN (2013). Modification of TiO(2) nanotube surfaces by electro-spray deposition of amoxicillin combined with PLGA for bactericidal effects at surgical implantation sites. *Acta Odontol Scand* 71(1): 168-174.

Malkoc S, Ozturk F, Corekci B, Bozkurt BS, Hakki SS (2012). Real-time cell analysis of the cytotoxicity of orthodontic mini-implants on human gingival fibroblasts and mouse osteoblasts. *Am J Orthod Dentofacial Orthop* 141(4): 419-426.

Meredith DO, Riehle MO, Curtis ASG, Richards RG (2007). Is surface chemical composition important for orthopaedic implant materials? *J Mater Sci Mater Med* 18(2): 405-413.

Moulder JF, Chastain J (1992). Handbook of x-ray photoelectron spectroscopy : a reference book of standard spectra for identification and interpretation of XPS data Eden Prairie: Physical Electronics Division, Perkin-Elmer Corp.

Park J, Bauer S, von der Mark K, Schmuki P (2007). Nanosize and vitality: TiO2 nanotube diameter directs cell fate. *Nano Lett* 7(6):1686-1691.

Rupp F, Scheideler L, Olshanska N, de Wild M, Wieland M, Geis-Gerstorfer J (2006). Enhancing surface free energy and hydrophilicity through chemical modification of microstructured titanium implant surfaces. *J Biomed Mater Res A* 76A(2): 323-334.

S Oh, KS Brammer, YSJ Li, D Teng, A Engler S Chien S Jin (2009). Stem

cell fate dictated solely by altered nanotube dimension. *National Acad Sciences* 106(7): 2130-2135.

Sawase T, Jimbo R, Baba K, Shibata Y, Ikeda T, Atsuta M (2008). Photo-induced hydrophilicity enhances initial cell behavior and early bone apposition. *Clin Oral Implants Res* 19(5): 491-496.

Schwarz F, Sager M, Ferrari D, Herten M, Wieland M, Becker J (2008). Bone regeneration in dehiscence-type defects at non-submerged and submerged chemically modified (SLActive) and conventional SLA titanium implants: an immunohistochemical study in dogs. *J Clin Periodontol* 35(1): 64-75.

Shibata Y, Hosaka M, Kawai H, Miyazaki T (2002). Glow Discharge Plasma Treatment of Titanium Plates Enhances Adhesion of Osteoblast-like Cells to the Plates Through the Integrin-Mediated Mechanism. *Int J Oral Maxillofac Impalnts* 17(6): 771-777.

Thierry B1, Tabrizian M, Savadogo O, Yahia L (2000). Effects of sterilization processes on NiTi alloy: surface characterization. *J Biomed Mater Res* 49(1):88-98.

Uhm SH, Song DH, Kwon JS, Lee SB, Han JG, Kim KM, Kim KN (2013). E-beam fabrication of antibacterial silver nanoparticles on diameter-controlled TiO_2 nanotubes for bio-implants. *Surf Coat Technol* 228 (1): S360-S366.

Uhm SH, Song DH, Kwon JS, Lee SB, Han JG, Kim KN (2014). Tailoring of antibacterial Ag nanostructures on TiO2 nanotube layers by magnetron sputtering. *J Biomed Mater Res B Appl Biomater* 102(3): 592-603.

Ungvari K, Pelsoczi IK, Kormos B, Oszko A, Rakonczay Z, Kemeny L, et al. (2010). Effects on titanium implant surfaces of chemical agents used for the treatment of peri-implantitis. *J Biomed Mater Res B Appl Bio*mater 94(1): 222-229.

Vezeau PJ, Koorbusch GF, Draughn RA, Keller JC (1996). Effects of multiple sterilization on surface characteristics and in vitro biologic responses to titanium. *J Oral Maxillofac Surg* 54(6): 738-746.

Walter MS, Frank MJ, Sunding MF, Gomez-Florit M, Monjo M, Bucko MM, et al. (2013). Increased reactivity and in vitro cell response of titanium based implant surfaces after anodic oxidation. *J Mater Sci Mater Med* 24(12): 2761-2773.

Wennerberg A, Albrektsson T (2010). On implant surfaces: a review of current knowledge and opinions. *Int J Oral Maxillofac Implants* 25(1): 63-74.

Wirth C, Brigitte Grosgogeat B, Lagneau C, Jaffrezic-Renault N, Ponsonnet L (2008). surface properties modulate in vitro rat calvaria osteoblasts response: Roughness and or chemistry? *Mater Sci Eng*: C 28(5-6): 990-1001.

Yamamoto H, Shibata Y, Miyazaki T (2005). Anode glow discharge plasma treatment of titanium plates facilitates adsorption of extracellular matrix proteins to the plates. *J Dent Res* 84(7): 668-671.

Zhao G, Schwartz Z, Wieland M, Rupp F, Geis-Gerstorfer J, Cochran DL, et al. (2005). High surface energy enhances cell response to titanium substrate microstructure. *J Biomed Mater Res* A 74(1): 49-58.

ABSTRACT (IN KOREAN)

질소 및 공기 상온대기압 플라즈마가 나노튜브 표면의 세포활성에 미치는 영향

< 지도교수 김경남 >

연세대학교 치의학과

서 혜 연

임플란트 주재료인 티타늄의 표면형태와 작용하는 화학기는 성공적인 골유착에 중요한 요소이다. 세포부착 시 임플란트 표면의 형태보다 화학기가 더 큰 영향을 미친다. 화학기 변화를 유도하는 한 가지 방법인 플라즈마 조사는 임플란트 표면을 친수성으로 개질하여 주변 조직의 세포와 단백질 흡착에 도움을 준다.

그러나 임플란트 표면개질을 유도하기 위한 화학기 변화는 시간이 지남에 따라 화학적 손실(aging)을 일으키기 쉽다. 이에 임플란트 개봉 즉시 표면개질을 유도할 수 있는 상온대기압 플라즈마(Non-thermal Atmospheric Pressure Plasma Jet; NTAPPJ)를 이용하여 화학처리가 손실되는 것을

최소화하고자 한다.

한편 다양한 표면형태 가운데 나노구조는 세포의 증식과 분화를 촉진하여 골 유착에 탁월한 효과가 있다. 따라서 본 연구는 나노튜브 표면 형태와 조도 변화없이 친수성으로 표면개질하여 골유착을 유도하는 것이 최종목표이다.

시편 위에 NTAPPJ를 처리한 전/후 표면의 물리적, 화학적, 생물학적 특성 변화는 전계방출 주사전자 현미경, 광학적 표면조도 측정기, 접촉각 및 X선 광전자분광 장치를 사용하여 측정 하였다. Mouse fibroblast L929로 세포생존, 조골모세포주(MC3T3-E1)를 배양하여 세포부착 및 증식, 세포분화는 Rat Mesenchymal Stem Cells을 사용하여 real-time PCR로 평가 하였다.

질소와 공기 기반의 NTAPPJ조사 시 두 실험군 모두 나노튜브의 형태 및 조도 변화는 없었다($P>0.05$). 접촉각 측정결과는 실험군 모두 대조군에 비하여 접촉각이 낮았으며, 질소 그룹이 공기 그룹에 비하여 측정값이 더 낮아 초친수성으로 표면이 개질되었다($P<0.05$).

NTAPPJ조사 후 표면층에 남아있는 원소를 XPS로 분석한 결과 O-H 그룹의 결합에너지가 다소 증가하였으며, COOH, NH그룹의 결합에너지는 급격하게 증가하였다.

세포부착과 증식률은 NTAPPJ조사 후 실험군이 대조군에 비하여 증가하였으며, 3일차부터 질소 그룹이 공기 그룹에 비하여 증식률이 더 높았다($P<0.05$). 모든 골아세포의 분화 표지인자에서 NTAPPJ 반응 시 유전자 발현이 증가하였으며, 배양한지 7일에서 14일까지 점점 증가하는 양상이

나타났다. 14일차에서 질소그룹이 공기 그룹에 비하여 발현이 유의하게 높았다($P<0.05$).

시편 위에 NTAPPJ 조사 시 실험군 모두 세포의 부착, 증식 및 분화가 촉진되었으며, 질소 그룹이 공기 그룹 보다 골 형성 유전자 발현이 높았다. 그 이유는 질소-NTAPPJ를 조사하였을 때, 표면의 탄소 원자 비율이 더 낮아지면서 표면에너지가 증가하였기 때문이다.

본 연구는 나노튜브 표면에 NTAPPJ를 조사한 결과 친수성이 증가하였으며, 성공적인 골 유착을 유도하였다.

핵심 되는 말 : 상온 대기압 플라즈마, 나노튜브, 골유착, 질소, 공기